



**Abstract:**

33 Fram Strait is the primary pathway for sea ice export from the Arctic Ocean yet  
34 estimates of volume export are constrained by observations of ice thickness and drift. Using  
35 a new year-round CryoSat-2 ice thickness product we determine an average annual export  
36 of  $1,712 \pm 452 \text{ km}^3$  from 2011-2022. 15% of the Arctic Oceans sea ice volume is exported  
37 annually, while 3.2% of the volume lost during the melt season is exported. Comparing high-  
38 and low-resolution ice drift products reveals the latter underestimate export by 30%.  
39 Comparing volume export between  $82^\circ\text{N}$  and  $79^\circ\text{N}$  reveals a high melt rate of  $1 \text{ cm d}^{-1}$ ,  
40 reducing export by 53%. September sea ice volume declines by  $286 \text{ km}^3$  for every  $100 \text{ km}^3$   
41 exported during summer, highlighting how export amplifies the ice-albedo feedback. Our  
42 estimates of volume export provide new insight into Fram Straits role as a sea ice sink and  
43 freshwater source.

**Plain Language Summary:**

44  
45  
46 Sea ice in the Arctic Ocean is either lost through melt or export. Fram Strait is the  
47 primary pathway for sea ice export, yet t estimates of sea ice volume export are limited by  
48 the availability of ice thickness and drift data. Here we use a new year-round record of ice  
49 thickness from the satellite altimeter CryoSat-2 to refine the estimates of sea ice volume  
50 export from 2011 to 2022. Overall, we find that  $1,712 \text{ km}^3$  or approximately 15% of the sea  
51 ice in the Arctic Ocean is exported annually. Calculating ice volume export at different  
52 locations reveals high melt rates in the area that thin the ice as it drifts south towards the  
53 north Atlantic Ocean. These estimates are not only key to understanding sea ice loss in the  
54 Arctic Ocean but also the supply of freshwater to the north Atlantic, where overturning is  
55 critical to the global climate.

56

**57 1. Introduction:**

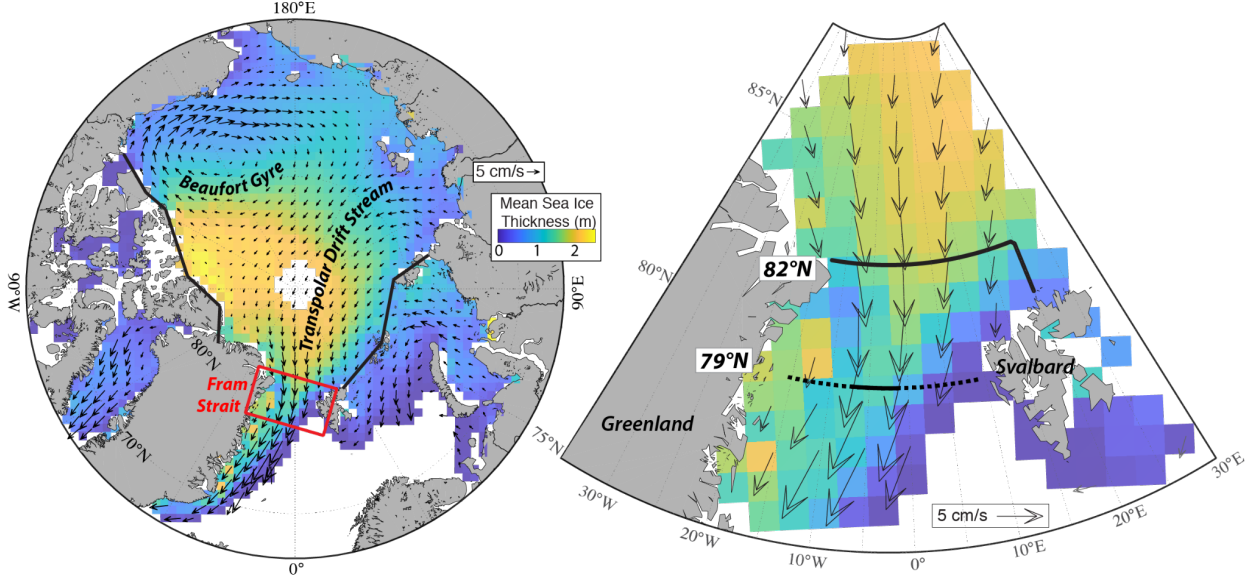
58 Fram Strait is the primary pathway for sea ice export from the Arctic Ocean. As a  
59 result, it plays a significant role in both the ice mass balance of the Arctic Ocean and the  
60 delivery of freshwater to the North Atlantic, where it impacts the Atlantic meridional  
61 overturning circulation (Belkin et al., 1998; Ionita et al., 2016). Sea ice export through Fram  
62 Strait removes approximately 10% of the sea ice area (Smedsrud et al., 2017) and 14% of  
63 the sea ice volume in the Arctic Ocean annually (Spren et al., 2020), while also comprising  
64 25% of the total freshwater delivered to the North Atlantic (Lique et al., 2009). Sea ice is  
65 advected towards Fram Strait by the Transpolar Drift Stream (Figure 1A) while the sea level  
66 pressure gradient across the Strait dictates wind speeds, which drive ice drift and therefore  
67 ice flux through the Strait. This gradient drives a pronounced annual cycle in sea ice export  
68 from a peak in March to a minimum in August (Smedsrud et al., 2017; Spren et al., 2020;  
69 Vinje et al., 1998). On average, between 706,000 and 880,000 km<sup>2</sup> of sea ice is exported  
70 through Fram Strait annually (Kwok, 2009; Smedsrud et al., 2017), however scaling this to  
71 sea ice volume export has been limited by the availability of ice thickness data.

72 Historically, sea ice volume export has been examined along a flux gate at 79°N where  
73 moored Upward Looking Sonars (ULS) have provided year-round observations of sea ice  
74 thickness since 1990 (Figure 1B). Initial estimates in the 1990s varied between 2,218 and  
75 2,850 km<sup>3</sup> per year (Kwok, 2004; Kwok & Rothrock, 1999; Vinje et al., 1998). More recently,  
76 Spren et al. (2020) determined an average annual volume export of 2,400 km<sup>3</sup> from 1992-  
77 2014 but found that a reduction in ice thickness (-15% per decade) has driven a reduction  
78 in sea ice volume export (-27% per decade). In particular, the ULS have revealed a reduction  
79 in the thickness of multi-year sea ice and presence of deformed ice in Fram Strait (Hansen et  
80 al., 2013), while there was a particular shift towards younger thinner ice passing through  
81 Fram Strait around 2007 (Babb et al., 2023; Sumata et al., 2023). Overall, annual average sea  
82 ice volume export, as estimated from the ULS, has declined from 2,450 km<sup>3</sup> in the 1990s, to  
83 1,760 km<sup>3</sup> in the 2000s and 1,390 km<sup>3</sup> from 2010-2017, with a minimum of 590 km<sup>3</sup> in 2018  
84 (Sumata et al., 2022). The disparity between the long-term negative trend in volume export  
85 and positive trend in area export (Smedsrud et al., 2017) highlights the importance of sea ice  
86 thickness observations.

87           While the ULS provide high resolution observations of ice thickness year-round, they  
88 are limited by their spatial coverage (7°W - 3°W; Figure 1B) and therefore require thickness  
89 to be extrapolated across the gate, which leads to significant uncertainty in volume flux  
90 estimates (i.e., 26% to 44%; Sumata et al., 2023). Conversely, satellite altimetry does not  
91 offer the high temporal resolution of a ULS but does provide complete coverage across the  
92 flux gate. Furthermore, the location of flux gates can be changed when using altimeters,  
93 which provides insight into local changes to the ice pack (i.e., melt) and can offer greater  
94 precision at higher latitudes where overpasses are more frequent (i.e., 82°N; Ricker et al.,  
95 2018). The limitation with altimeters is that historically they only provided estimates of  
96 thickness during winter (October to April), when the ice surface is cold. Using ICESat, Spreen  
97 et al., (2009) estimated an average winter export of 1,564 km<sup>3</sup> at 80°N from 2003-2008,  
98 though this estimate relied on ULS to fill gaps between the two ICESat observing periods  
99 (October-November and February-March). Using CryoSat-2, Ricker et al., (2018) estimated  
100 an average winter export of 1,711 km<sup>3</sup> at 82°N from 2010 to 2017. However, despite a  
101 majority of sea ice export occurring during winter, there was a summer gap in satellite  
102 estimates. Krumpfen et al., (2016) used sparse airborne ice thickness surveys to estimate an  
103 average monthly export of 17 km<sup>3</sup> during July and August. However, there remains a gap  
104 during spring (May and June) when ice drift speeds remain modest, and a significant volume  
105 of sea ice may still be exported.

106           Here we use new year-round estimates of ice thickness from CryoSat-2 (Landy et al.,  
107 2022) in combination with a passive microwave ice drift product to close the annual record  
108 of sea ice volume export through Fram Strait from 2010-2022. We further refine estimates  
109 of volume export from 2016-2022 using high resolution observations of ice drift from  
110 spaceborne synthetic aperture radar (SAR) imagery. We discuss the consistency between  
111 published estimates of the volume flux, including the impact of selecting gates over the ULS  
112 array at 79°N or further north. Finally, we consider the role of sea ice volume export through  
113 Fram Strait in modulating the ice mass balance of the Arctic Ocean and the delivery of  
114 freshwater to the North Atlantic.

115  
116  
117



118  
 119 Figure 1: Mean fields of sea ice thickness and drift from 2010-2022 across the Arctic Ocean  
 120 (left) and in the vicinity of Fram Strait (right) with the two gates at 82°N and 79°N presented.  
 121 The Arctic Ocean for the ice mass balance analysis is defined by the black lines in the pan-  
 122 Arctic map along with the Bering Strait and the chosen gate at Fram Strait. In the Fram Strait  
 123 panel, the solid portion of the 79°N gate between 3° and 7°W is where the ULS are located.

124

125 **2. Methods:**

126 Sea ice volume flux ( $F$ ) through Fram Strait ( $\text{km}^3 \text{d}^{-1}$ ) was calculated at 44 intervals  
 127 ( $i$ ) along the 82°N flux gate (Figure 1) previously used by Ricker et al., (2018).  $F$  was  
 128 calculated using the following equation,

129  
 130 
$$F_i = \sum_{i=1}^n (C_i H_i u_i \Delta x) \tag{1}$$

131  
 132 where  $C$  is fractional sea ice concentration,  $H$  is ice thickness (km),  $u$  is ice drift speed normal  
 133 to the gate ( $\text{km d}^{-1}$ ) and  $\Delta x$  is the interval (15 km). Positive values of  $F$  indicate sea ice export  
 134 from the Arctic Ocean, while negative values indicate ice import into the Arctic Ocean.  $C$ ,  $H$   
 135 and  $u$  were interpolated from gridded products to each interval at each time step.  $F$  is  
 136 summed annually from October to September.

137 Year-round fields of  $H$  from CryoSat-2 are provided at bimonthly intervals from  
 138 October 2010 to July 2022 (Landy & Dawson, 2022).  $H$  is generally thinner in this product  
 139 than the Alfred Wegener Institute (AWI) product used by Ricker et al., (2018) due to

140 differences in radar echo re-tracking (described in Landy et al. (2020)), and snow loading.  
 141 The AWI product uses a modified Warren (1999) snow climatology, whereas Landy and  
 142 Dawson (2022) uses the Lagrangian snow evolution scheme SnowModel-LG (Liston et al.,  
 143 2020; Stroeve et al., 2020). Validating their product against the ULS in Fram Strait, Landy et  
 144 al. (2022) found a mean bias of +11 cm.

145 For the full CryoSat-2 record,  $F$  was calculated from fields of sea ice concentration  
 146 (Cavalieri et al., 1996; updated 2023) and motion (Tschudi et al., 2019; updated 2023)  
 147 derived from spaceborne passive microwave sensors. These estimates are referred to as  
 148  $F_{PMW}$ . For comparison to previous studies,  $F_{PMW}$  was also calculated at 79°N. Sea ice area flux  
 149 ( $\text{km}^2$ ) was calculated by solving  $F_{PMW}$  without  $H$ .

150  $F$  was also calculated from 2016-2022 using high spatiotemporal resolution ice drift  
 151 data (i.e., ~1 day, 200 m) derived from a combination of spaceborne SAR imagery (i.e.,  
 152 Sentinel-1, RADARSAT-2 and RADARSAT Constellation Mission) using the methodology of  
 153 Komarov and Barber (2014) and ice concentration from daily ice charts from the National Ice  
 154 Center (U.S. National Ice Center, 2023). These estimates are referred to as  $F_{SAR}$ . SAR resolves  
 155 faster ice drift speeds than passive microwave drift products (Howell et al., 2022; Kwok et  
 156 al., 1998; Smedsrud et al., 2017), which is important in Fram Strait where the fastest ice drift  
 157 in the Arctic Ocean occurs (Figure 1).

158 Following Ricker et al., (2018) the uncertainty of  $F_{PMW}$  ( $\sigma F_{PMW}$ ) at each interval and  
 159 time step, assuming uncorrelated errors between variables, is determined with the following  
 160 equation,

$$161 \quad \sigma F_{PMW} = L \sqrt{(H C \sigma_u)^2 + (H \sigma_C u)^2 + (\sigma_H C u)^2} \quad (2)$$

162  
 163 where,  $\sigma H$ ,  $\sigma C$  and  $\sigma u$  are the uncertainties in thickness, concentration and drift respectively,  
 164 and  $L$  is the length of the interval.  $\sigma C$  is set at 5% (Ricker et al., 2018).  $\sigma H$  is taken from the  
 165 CryoSat-2 product (Landy and Dawson, 2022) and has a mean of 0.32 m.  $\sigma u$  is taken from  
 166 Sumata et al., (2014) and set at 0.873  $\text{km d}^{-1}$  during winter (October-April) and 1.123  $\text{km d}^{-1}$   
 167 during summer (May-September). The monthly uncertainty at 82°N peaks in March and  
 168 April at 60  $\text{km}^3$  per month and is 17  $\text{km}^3$  during August and September. The average annual  
 169 uncertainty at 82°N and 79°N is 452  $\text{km}^3$  and 176  $\text{km}^3$ , which are equal to 26% and 21% of

170 the average annual fluxes, respectively. The uncertainty in  $F_{SAR}$  is lower as the error in SAR-  
171 derived ice motion is estimated to be  $0.43 \text{ km d}^{-1}$  (Komarov & Barber, 2014).

172 Sea ice volume flux is scaled by 0.8 to estimate liquid freshwater flux relative to a  
173 reference salinity of 34.8 (Haine et al., 2015). The contribution of snow to the freshwater flux  
174 was calculated by replacing  $H$  in equation 1 with snow depth from SnowModel-LG and then  
175 using snow density from the model to calculate the liquid equivalent ( $\text{km}^3$ ).

176

### 177 **3. Results and Discussion:**

#### 178 **3.1 Sea ice volume export at 82°N**

##### 179 3.1.1 Sea ice volume export

180 The biweekly record of  $F_{PMW}$  through Fram Strait is presented in Figure 2A. On  
181 average  $72 \text{ km}^3$  of sea ice was exported biweekly, with a peak of  $306 \text{ km}^3$  during late  
182 February 2012.  $F_{PMW}$  was only positive (import) during 22 biweekly periods (8%), most of  
183 which occurred between July and September, and all of which were below  $20 \text{ km}^3$  and  
184 therefore in the range of the monthly uncertainty. Similar to the annual record in sea ice area  
185 export, the annual cycle in volume export shows a peak in March ( $305 \text{ km}^3$ ) and minimum in  
186 August ( $19 \text{ km}^3$ ; Figure 2B; Table 1). The reduction during spring and summer is gradual, so  
187 although  $F_{PMW}$  from July to September is very low (4% of the annual flux),  $F_{PMW}$  during May  
188 and June, which have not been captured by previous altimeter or airborne estimates, make  
189 a significant contribution ( $\sim 15\%$ ) to the annual flux.

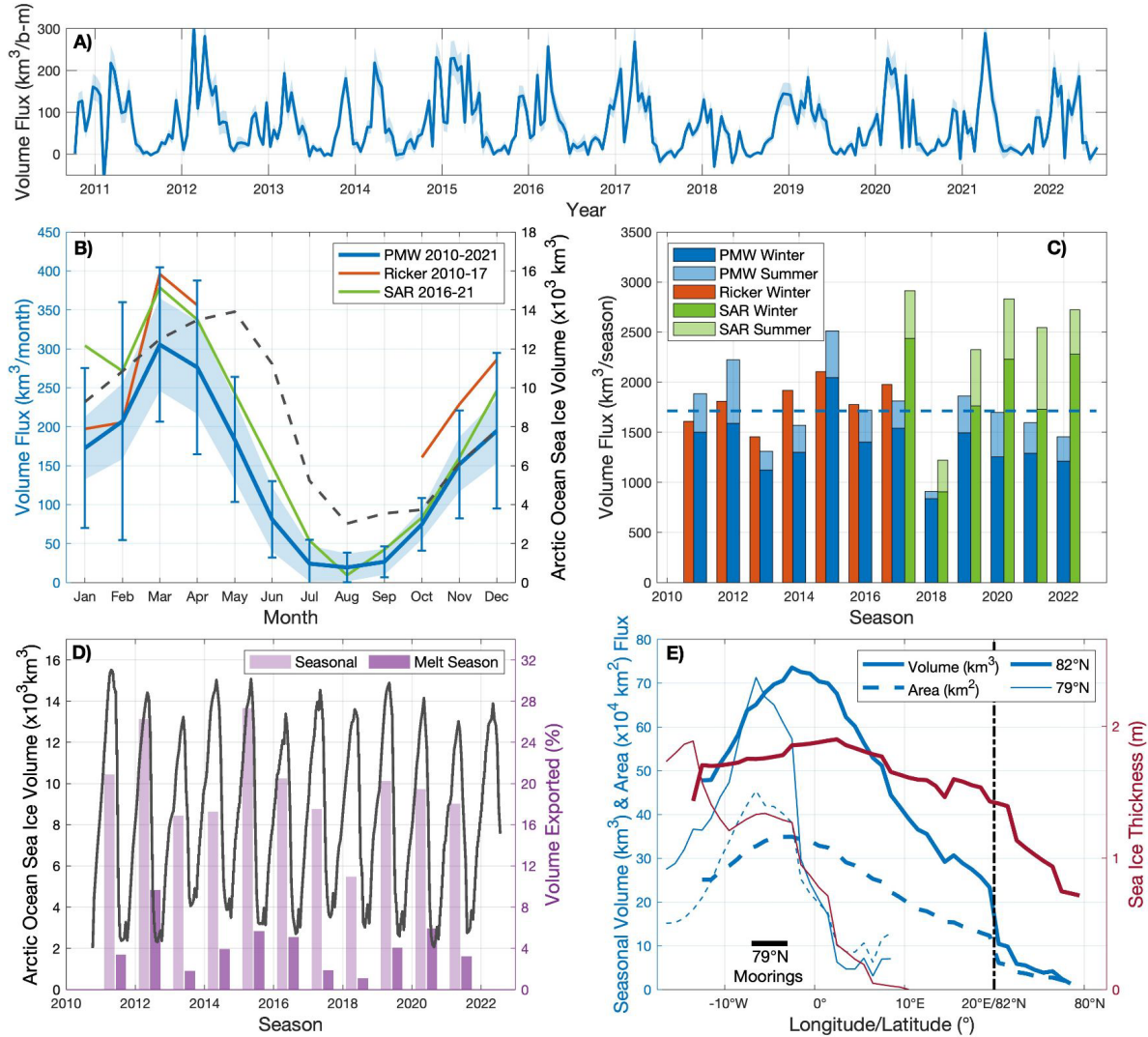
190 The monthly averages of  $F_{PMW}$  from winters 2010-2017 are 20% lower than those of  
191 Ricker et al., (2018) (orange in Figure 2B), which is expected given that our estimates of ice  
192 thickness are inherently thinner. Monthly averages of  $F_{PMW}$  from 2016-2022 are 27% lower  
193 than  $F_{SAR}$ , which is expected given that SAR detects faster ice drift speeds. These disparities  
194 highlight the importance of continuing to refine estimates of ice thickness and drift used to  
195 calculate volume fluxes. Furthermore, it provides important context on the interpretation of  
196 existing records of volume export derived from passive microwave drift products, which  
197 may underestimate volume export by nearly one-third.

198 Over the full CryoSat-2 record,  $F_{PMW}$  gives an average annual export of  $1,712 \text{ km}^3$   
199 through Fram Strait with a peak of  $2,512 \text{ km}^3$  in 2015 and minimum of  $907 \text{ km}^3$  in 2018  
200 (Figure 2C; Table 1). From 2016-2021,  $F_{SAR}$  gives an average annual export of  $2,360 \text{ km}^3$ , with

201 a peak of 2,914 km<sup>3</sup> in 2017 and minimum of 1,219 km<sup>3</sup> in 2018. Both datasets show a  
202 minimum in 2018 due to anomalously low export from February to May (Table 1), but also  
203 show a recovery in the years after, meaning 2018 did not provoke a step change in the  
204 volume flux but was rather an anomalously low year. There is no apparent linear trend in  
205 either  $F_{PMW}$  or  $F_{SAR}$ , although the records are too short for reliable climate signals to emerge.  
206 For comparison,  $F_{PMW}$  and  $F_{SAR}$  through Fram Strait are nearly seven- and ten-times greater,  
207 respectively, than the combined sea ice volume export through Nares Strait and the Canadian  
208 Arctic Archipelago (Howell et al., 2023).

209         Seasonally, 80% (76% in  $F_{SAR}$ ) of the volume export occurs during winter (October-  
210 April) while the remaining 20% (24%) occurs during summer (May-September) and  
211 represents the gap that year-round observations of ice thickness can fill. On average 360 km<sup>3</sup>  
212 was exported during summer, with a peak of 633 km<sup>3</sup> in 2012 and minimum of 71 km<sup>3</sup> in  
213 2018. Although the standard deviation of volume flux during winter is greater than summer  
214 (305 vs 149 km<sup>3</sup>), the coefficient of variation for summer (44%) is double that for winter  
215 (22%), indicating volume export is twice as variable during summer compared to winter.  
216 Examining the contribution of concentration, drift, and thickness to the significant change in  
217 variance between summer and winter we find that it is primarily due to the seasonal change  
218 in ice drift. The coefficient of variation for ice drift increases from 79% in winter to 131% in  
219 summer, compared to a negligible change in the contribution of concentration from 35% in  
220 winter to 36% in summer, and a slight increase in the contribution of thickness from 55% in  
221 winter to 63% in summer. Similarly, Ricker et al., (2018) found that a majority of the  
222 variability in winter volume flux was due to variability in ice drift.

223



224  
 225 Figure 2: Sea ice volume export at 82°N. A) bi-weekly record of  $F_{PMW}$ . B) Monthly cycle of  
 226  $F_{PMW}$  (2010-2022; blue),  $F_{SAR}$  (2016-2022; green) and  $F$  from Ricker et al., (2018; 2010-2017;  
 227 orange) with the monthly cycle of sea ice volume in the Arctic Ocean (gray dashed). The  
 228 shading in A) and B) represent the uncertainty in  $F_{PMW}$ . The error bars in B) represent the  
 229 standard deviation in monthly  $F_{PMW}$ . C) Annual  $F_{PMW}$  from 2011-2022 decomposed by winter  
 230 (October to April) and summer (May to September) compared against winter fluxes from  
 231 Ricker et al., (2018; orange) and year-round  $F_{SAR}$  (green). The dashed line in C) shows the  
 232 mean annual  $F_{PMW}$ . D) bi-weekly record of sea ice volume in the Arctic Ocean and the  
 233 proportion (%) exported through Fram Strait annually and each melt season. E) Across-  
 234 Strait profile of the mean annual sea ice area and volume fluxes per year, and the mean ice  
 235 thickness at each interval (1° longitude at 82°N or 15 km). In E) the thick lines denote data  
 236 for 82°N, the thin lines denote data for the 79°N, the vertical dashed line denotes the switch  
 237 from a zonal to meridional gate along the 82°N gate and the thick black line shows the  
 238 longitudinal span of the 79°N mooring array.

239 Table 1: Monthly sea ice volume flux (km<sup>3</sup>) through Fram Strait (82°N) from October 2010  
 240 to July 2022. The monthly mean and annual sum are presented along their respective rows  
 241 and columns. SAR estimates of sea ice volume flux are provided in brackets from February  
 242 2016 to July 2022.

Month	Year													Mean
	2010	2011	2012	2013	2014	2015	2016	2017	2018	2019	2020	2021	2022	
Jan		295	54	75	32	151	85	358 (488)	206 (279)	244 (284)	118 (233)	152 (206)	300 (333)	173 (304)
Feb		-20	457	108	94	457	259 (42)	115 (266)	77 (17)	201 (193)	364 (723)	68 (78)	301 (582)	207 (271)
Mar		416	277	295	283	410	337 (194)	430 (474)	122 (125)	293 (400)	395 (740)	286 (399)	119 (318)	305 (379)
Apr		248	464	246	338	312	263 (93)	272 (412)	106 (117)	181 (234)	149 (269)	503 (727)	232 (510)	276 (337)
May		252	303	115	111	202	152 (130)	239 (251)	-19 (101)	205 (284)	206 (323)	222 (393)	212 (221)	183 (243)
Jun		101	149	41	40	164	54 (21)	47 (171)	70 (143)	102 (147)	153 (196)	36 (270)	16 (100)	81 (150)
Jul		19	95	27	1	63	39 (6)	-24 (36)	-9 (11)	5 (29)	34 (58)	23 (115)	17 (122)	24 (54)
Aug		3	34	8	62	8	48 (10)	10 (9)	4 (1)	13 (30)	6 (-1)	16 (6)		19 (9)
Sep		8	53	-3	56	30	29 (56)	-1 (11)	25 (58)	40 (73)	45 (27)	8 (28)		27 (42)
Oct	125	52	108	106	130	31	72 (101)	68 (58)	73 (149)	60 (47)	43 (39)	25 (104)		75 (83)
Nov	182	84	143	315	147	181	68 (166)	119 (110)	215 (201)	43 (74)	147 (104)	175 (306)		152 (160)
Dec	255	203	146	130	439	243	224 (530)	137 (199)	288 (300)	123 (141)	90 (180)	58 (126)		195 (246)
Sum		1884	2223	1310	1570	2512	1722	1811 (2914)	907 (1219)	1861 (2326)	1696 (2832)	1594 (2545)	1455 (2722)	

243

### 244 3.1.2 Sea ice volume export and the Arctic Ocean ice mass balance

245 Comparing the biweekly record of  $F_{PMW}$  and total sea ice volume within the Arctic  
 246 Ocean (Figure 2D - boundaries in Figure 1A) we quantify the contribution of volume export  
 247 through Fram Strait to the sea ice mass balance of the Arctic Ocean. Between 2011 and 2022,  
 248 an average of 14.6% of the sea ice volume in the Arctic Ocean was exported through Fram  
 249 Strait annually (Figure 2E). This is similar to the 14% reported by Spreen et al., (2020) using  
 250 ULS data for export and PIOMAS for sea ice volume from 1992-2014 and implies that this  
 251 proportion has been relatively stable over the last 30 years. This might be expected given  
 252 that both sea ice volume in the Arctic Ocean and export through Fram Strait have declined at  
 253 respective rates of -15% per decade (Kwok, 2018) and -27% per decade (Spreen et al., 2020).  
 254 The proportion peaked at 21.8% in 2012, when volume export was the second highest of the  
 255 study period and fell to a minimum of 7.4% in 2018. For comparison, over the same period  
 256 11% of the sea ice area in the Arctic Ocean was exported through Fram Strait annually,  
 257 highlighting the higher-than-average thickness of ice passing through Fram Strait.

258           During summer, sea ice volume export through Fram Strait explained only 3.2% of  
259 the average 10,400 km<sup>3</sup> of sea ice lost from the Arctic Ocean between May and September  
260 (Figure 2B). For comparison, 5% of the reduction in sea ice area was due to export. Fram  
261 Strait has a lower impact on summer volume loss than area loss because volume and area  
262 are both lost from ice that melts out completely, while volume is also lost from ice that  
263 persists through September. The contribution of sea ice export to the loss of sea ice during  
264 summer peaked at 5.5% in 2012, when summer volume export peaked and contributed to  
265 the record sea ice minimum (Zhang et al., 2013), and was below 1% in 2018, when volume  
266 export was anomalously low (77 km<sup>3</sup>). Interestingly, summer volume export was only 2%  
267 during 2013 and 2017, which were both years of recovery following years of record sea ice  
268 loss.

269           Overall, summer sea ice volume export is found to be significantly correlated with  
270 September sea ice volume in the Arctic Ocean ( $r = -0.68$ ,  $p < 0.05$ ), while the relationship  
271 between annual export and September volume was not significant. Based on this  
272 relationship, September sea ice volume declines by 286 km<sup>3</sup> for every 100 km<sup>3</sup> exported  
273 during summer, the relationship is not one-to-one as export amplifies other feedbacks that  
274 in turn drive ice melt (i.e., ice-albedo feedback). Given the high degree of uncertainty in  
275 volume flux estimates, we test the robustness of this relationship by running 1000 iterations  
276 with random uncertainties drawn from a normal distribution of the summer flux uncertainty  
277 ( $\overline{\sigma F_S} = 148 \text{ km}^3$ ) applied to summer estimates of volume export. The relationship  
278 remained significant in 80% of the iterations, suggesting a robust negative relationship  
279 between summer volume export and September volume. A similar test with the annual  
280 volume export and September sea ice volume resulted in a significant negative relationship  
281 in only 2.5% of the iterations, supporting our finding of no relationship between the two.  
282 This implies that years with higher winter sea ice export do not precondition the Arctic's sea  
283 ice cover in spring for higher-than-normal melt and anomalously low September sea ice  
284 volume. High winter export may be offset by an enhanced negative thin ice-thermodynamic  
285 growth feedback (Stroeve et al., 2018).

286

287 3.1.3 Across Strait profiles

288 Satellite altimeters offer unique insight into the across-strait profile in ice thickness  
289 not captured by the ULS. Figure 2E shows the average across strait profiles in ice thickness,  
290 and the annual sea ice area and volume fluxes at 82°N and 79°N. At 82°N thickness is  
291 approximately 1.7 m near Greenland with a peak of 1.9 m around 2°E, a reduction towards  
292 1.5 m across the zonal gate before falling below 0.7 m along the meridional gate. Sea ice area  
293 flux between 2010 and 2022 peaked at 3°W and fell off quickly across the zonal gate with  
294 minimal export across the meridional gate as the normal component of the ice drift in this  
295 area is minimal. As the compound of the ice thickness and area flux profiles, the sea ice  
296 volume flux peaked at 3°W and declined across the zonal gate with very little volume being  
297 exported across the meridional gate. Export peaks in this area because of the East Greenland  
298 Current driving greater ice drift speeds (Ricker et al., 2018; Figure 1).

299

### 300 **3.2 Comparison between 82°N and 79°N and previous estimates.**

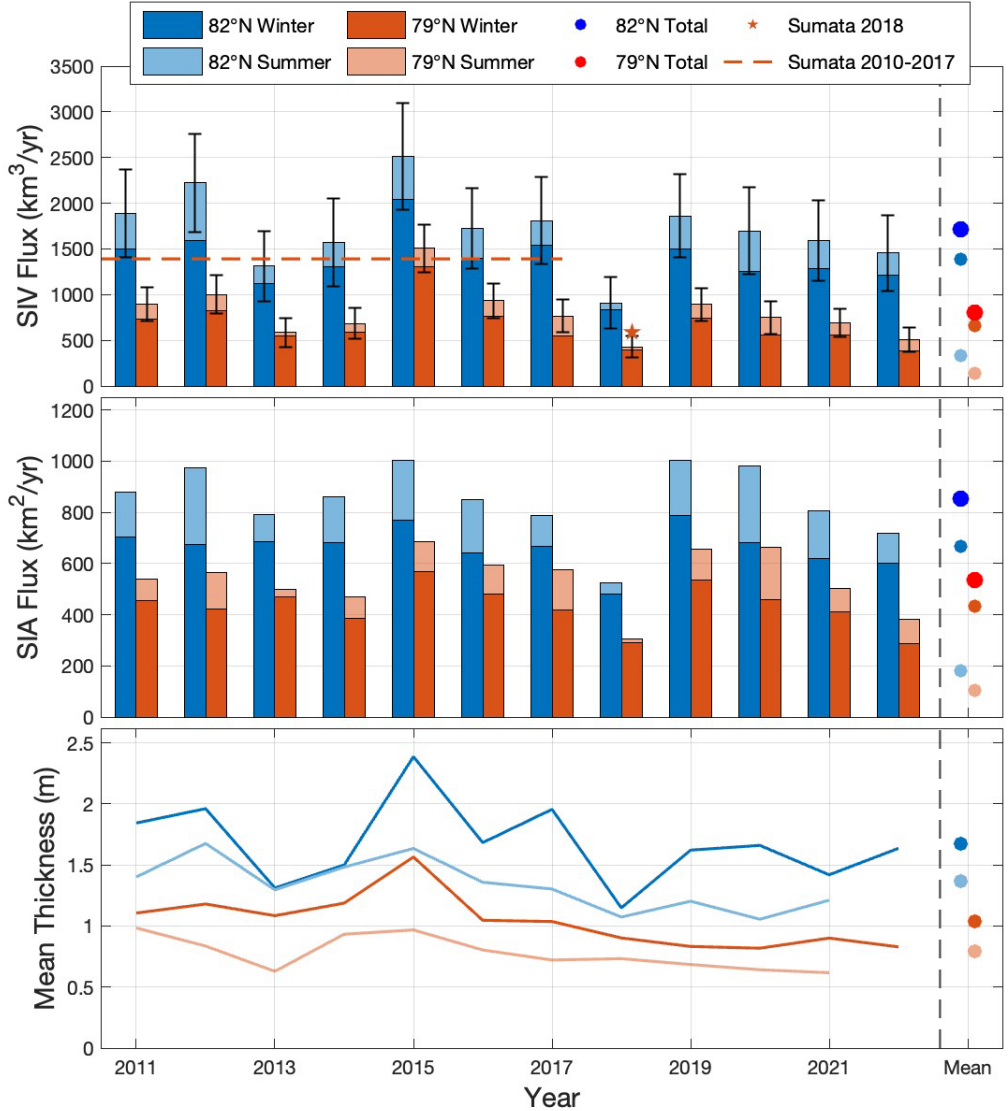
301  $F_{PMW}$  declined by 52% between 82°N and 79°N, with a slightly greater decrease during  
302 summer (58%) than winter (51%) (Figure 3). Reductions in both sea ice area flux (-36%)  
303 and thickness (-38%) drive the overall reduction in volume flux. The reduction in area flux  
304 is greater than the 10% reduction between 82°N and 79°N reported by Spreen et al., (2020),  
305 though their gates were oriented differently, and their study extended back to 1992, meaning  
306 that our observations could highlight a recent increase in the amount of sea ice area lost  
307 between these two gates. The reduction in area flux is primarily the result of a contraction  
308 of sea ice towards the Greenlandic coast (Figure 1B; 2E), however, this contraction does not  
309 represent ice convergence, as the ice thickness also declines between the gates. On average  
310 ice thickness declined by 0.20 m per degree-latitude between the gates, which was fairly  
311 consistent between winter (-0.20 m) and summer (-0.18 m) and agrees with the thinning  
312 rate of 0.19 m per degree-latitude observed during summer by Krumpfen et al., (2016). Given  
313 that the gates are separated by 333 km and the average drift speed over the two gates  
314 throughout the CryoSat-2 period is 5.6 km d<sup>-1</sup>, it takes an average of 59 days for the ice to  
315 drift from 82°N to 79°N. With an average thinning of 0.60 m between the gates over the full  
316 CryoSat-2 period, this equates to nearly 1 cm of melt per day throughout the year as the ice  
317 drifts between the two gates. Similarly, Sumata et al., (Duarte et al., 2020; Provost et al., 2017;  
318 Sirevaag & Fer, 2009; 2022) estimated high melt rates between 0.43 and 2.2 cm d<sup>-1</sup>

319 immediately upstream of their flux gate at 79°N using altimetry-based estimates of ice  
320 thickness along backward trajectories of the ice passing by the ULS. These high melt rates  
321 highlight the influence of warm Atlantic water in Fram Strait driving rapid ice melt in the  
322 vicinity of Fram Strait (i.e., Duarte et al., 2020; Sirevaag and Fer, 2009; Provost et al., 2017).

323 Our estimates of  $F_{PMW}$  at 79°N are routinely lower than previous estimates at this gate  
324 (i.e., Kwok & Rothrock, 1999; Spreen et al., 2020; Sumata et al., 2022; Vinje et al., 1998). The  
325 difference with historic estimates from the 1990s is primarily due to the transition towards  
326 a younger, thinner ice pack passing through Fram Strait (i.e., Babb et al., 2023; Sumata et al.,  
327 2023). However, focusing on the period from 2010-2018, our estimates are 33% less than  
328 those from Sumata et al., (2022). This difference is likely to be caused by the high degree of  
329 uncertainty associated with extrapolating the across-Strait thickness profile from ULS that  
330 cover only 85 of the 588 km across the 79°N gate, which may overestimate ice thickness  
331 (Figure 2E). It may also be caused by CryoSat-2 underestimating the thickness of very thick  
332 and rough ice floes in Fram Strait; however, CryoSat-2 overestimated the ULS ice thickness  
333 by 11 cm when the observations were directly compared (Landy et al., 2022).

334

335



336  
 337 Figure 3: Annual sea ice volume (A) and area (B) fluxes and the mean annual ice thickness  
 338 (C) for the 82°N and 79°N flux gates. The mean for the winter, summer and annual fluxes,  
 339 along with the mean winter and summer thicknesses are presented on the far right of each  
 340 plot. The error bars in A) represent the annual uncertainty in  $F_{PMW}$  at 82°N and 79°N.  
 341 Estimates of sea ice volume flux at 79°N from Sumata et al., (2022) are provided in Panel A.  
 342

343 **3.3 Freshwater Export Through Fram Strait.**

344 In addition to serving as a sink for the ice mass balance of the Arctic Ocean, sea ice  
 345 export through Fram Strait provides a large source of freshwater to the North Atlantic. For  
 346 the sake of comparing the solid (sea ice and snow) and liquid components of the freshwater  
 347 export through Fram Strait, we focus on the flux gate at 79°N where the moorings provide a

348 long-term record of liquid freshwater export (Rabe et al., 2013; de Steur et al., 2009). Our  
349 estimates of  $F_{PMW}$  are equal to an annual average freshwater flux of 664 km<sup>3</sup> with an  
350 additional 17 km<sup>3</sup> of freshwater from snow, for a total solid freshwater flux of 681 km<sup>3</sup> yr<sup>-1</sup>  
351 during the 2010s. This is considerably lower than previous freshwater budgets have  
352 estimated (2,300 km<sup>3</sup> yr<sup>-1</sup> Serreze et al., 2006; 1900 km<sup>3</sup> yr<sup>-1</sup> Haine et al., 2015), because  
353 these estimates have been based on historic observations of a thicker ice pack and were  
354 subject to the increased uncertainty of extrapolating ULS observations across the full 79°N  
355 gate (i.e., Vinje et al., 1998). The solid freshwater flux is only 21% of the liquid freshwater  
356 flux observed at the moorings (3,160 km<sup>3</sup>; Rabe et al., 2013), though based on the increased  
357 melt rates between gates, we can estimate that up to 21% of this liquid freshwater flux is  
358 released as ice melts immediately upstream of 79°N. Furthermore, our estimate of solid  
359 freshwater flux through Fram Strait is double the estimated solid freshwater flux through  
360 Davis Strait (331 km<sup>3</sup> yr<sup>-1</sup>; Curry et al., 2014), which is the other pathway for sea ice export  
361 into the North Atlantic. Together Fram and Davis Straits provide approximately 1,012 km<sup>3</sup>  
362 yr<sup>-1</sup> of freshwater to the North Atlantic.

363         Given that there is no long-term trend in liquid freshwater flux through Fram Strait  
364 (Rabe et al., 2013), we suggest that the reduction in sea ice volume export (Spren et al.,  
365 2020; Sumata et al., 2022) has led to an overall reduction in the total annual delivery of  
366 freshwater to the North Atlantic through Fram Strait. The magnitude of the total freshwater  
367 flux is projected to change under a warming climate, with reduced sea ice export but  
368 potentially enhanced liquid freshwater export through Fram Strait because of enhanced  
369 freshwater storage within the Arctic Ocean (Haine et al., 2015; Holland et al., 2007).

370

### 371 **Conclusions:**

372         A new year-round record of sea ice thickness from CryoSat-2 is used to complete the  
373 annual record of satellite-based estimates of Arctic sea ice volume export through Fram  
374 Strait. Using a passive microwave ice drift product over the full CryoSat-2 period (2010-  
375 2022), we find an average annual (October to September) export of 1,712 km<sup>3</sup> ( $\pm 452$  km<sup>3</sup>)  
376 with 80% occurring during winter (October to April) and 20% during summer (May to  
377 September), the latter of which has not previously been captured by satellite altimeter-based  
378 studies. However, compared to volume export derived from high resolution observations of

379 ice drift from SAR imagery, we find that passive microwave estimates underestimate volume  
380 export by nearly one-third, suggesting many previous records of volume export have  
381 underestimated the magnitude of sea ice export.

382 In terms of the ice mass balance of the Arctic Ocean, 14.6% of the Arctic Oceans sea  
383 ice volume is exported through Fram Strait annually, while 3.2% of the sea ice volume lost  
384 during the melt season is through export. We find a robust significant negative relationship  
385 between summer sea ice volume export and September sea ice volume in the Arctic Ocean,  
386 which declines by 286 km<sup>3</sup> for every 100 km<sup>3</sup> exported. Comparing sea ice volume export  
387 between the northerly gate at 82°N and the historic flux gate at 79°N, we find a 52%  
388 reduction. This highlights high melt rates in the vicinity of Fram Strait, with a year-round  
389 thinning of approximately 1 cm d<sup>-1</sup> during the 60 days that it takes for ice to drift between  
390 the gates. Our estimates of volume export across 79°N are three to four times below previous  
391 estimates based on historic sea ice thickness observations, which highlights the long-term  
392 negative trend in ice thickness and therefore volume export through Fram Strait. We suggest  
393 the reduction in sea ice export is reducing the overall freshwater flux to the North Atlantic.  
394 Our estimated freshwater volume flux through 79°N is only 21% of the observed liquid  
395 freshwater flux across the same gate, though our results show that the same volume of  
396 freshwater may have been released through ice melt immediately upstream of the flux gate.  
397 Overall, we provide new estimates of sea ice volume flux through Fram Strait and its  
398 influence on the Arctic Oceans ice mass balance, its role as a source for freshwater to the  
399 North Atlantic, and importantly the uncertainty associated with previous estimates of this  
400 critical term.

401

**Acknowledgements:**

403 This work is a contribution to the Canada Excellence Research Chair (CERC) in Arctic Ice,  
404 Freshwater Marine Coupling and Climate Change held by D. Dahl-Jensen at the University of  
405 Manitoba. D. Babb and S. Kirillov are supported by the CERC. D. Babb, J. Ehn and J. Stroeve  
406 would like to acknowledge financial support from the Natural Sciences and Engineering  
407 Research Council of Canada (NSERC). J. Landy acknowledges support from the Research  
408 Council of Norway (RCN) INTERAAC project under grant #328957, from the ERC project  
409 SI/3D under grant #101077496, and from the Fram Centre program for Sustainable  
410 Development of the Arctic Ocean (SUDARCO) under grant #2551323. J. Stroeve is supported  
411 by the Canada 150 Research Chair Program.

412

**Data Availability Statement**

414 The year-round record of sea ice thickness from CryoSat-2 is available from Landy and  
415 Dawson (2022). Daily fields of sea ice concentration and motion as observed by passive  
416 microwave satellites are available from Cavalieri et al., (1996) and Tschudi et al., (2019),  
417 respectively. We are in the process of packaging up the SAR ice motion data and adding it to  
418 the following ECCC repository [https://crd-data-donnees-  
rdc.ec.gc.ca/CPS/products/IceFlux/](https://crd-data-donnees-<br/>419 rdc.ec.gc.ca/CPS/products/IceFlux/).

420 **References:**

- 421 Babb, D. G., Galley, R. J., Kirillov, S., Landy, J. C., Howell, S. E. L., Stroeve, J. C., et al. (2023).  
 422 The Stepwise Reduction of Multiyear Sea Ice Area in the Arctic Ocean Since 1980. *Journal*  
 423 *of Geophysical Research: Oceans*, 128(10), 1–19. <https://doi.org/10.1029/2023JC020157>
- 424 Belkin, I. M., Levitus, S., Antonov, J., & Malmberg, S.-A. (1998). “Great Salinity Anomalies” in  
 425 the North Atlantic. *Progress in Oceanography* (Vol. 41).
- 426 Cavalieri, D. J., Parkinson, C. L., Gloersen, P., & Zwally, H. J. (1996). *Sea Ice Concentrations*  
 427 *from Nimbus-7 SMMR and DMSP SSM/I-SSMIS Passive Microwave Data*. Boulder,  
 428 Colorado, USA.
- 429 Curry, B., Lee, C. M., Petrie, B., Moritz, R. E., & Kwok, R. (2014). Multiyear Volume, Liquid  
 430 Freshwater, and Sea Ice Transports through Davis Strait, 2004–10. *Journal of Physical*  
 431 *Oceanography*, 44(4), 1244–1266. <https://doi.org/https://doi.org/10.1175/JPO-D-13-0177.1>
- 432 Duarte, P., Sundfjord, A., Meyer, A., Hudson, S. R., Spreen, G., & Smedsrud, L. H. (2020).  
 433 Warm Atlantic Water Explains Observed Sea Ice Melt Rates North of Svalbard. *Journal of*  
 434 *Geophysical Research: Oceans*, 125(8). <https://doi.org/10.1029/2019JC015662>
- 435 Haine, T. W. N., Curry, B., Gerdes, R., Hansen, E., Karcher, M., Lee, C., et al. (2015, February  
 436 1). Arctic freshwater export: Status, mechanisms, and prospects. *Global and Planetary*  
 437 *Change*. Elsevier B.V. <https://doi.org/10.1016/j.gloplacha.2014.11.013>
- 438 Hansen, E., Gerland, S., Granskog, M. A., Pavlova, O., Renner, A. H. H., Haapala, J., et al.  
 439 (2013). Thinning of Arctic sea ice observed in Fram Strait: 1990-2011. *Journal of*  
 440 *Geophysical Research: Oceans*, 118(10), 5202–5221. <https://doi.org/10.1002/jgrc.20393>
- 441 Holland, M. M., Finnis, J., Barrett, A. P., & Serreze, M. C. (2007). Projected changes in Arctic  
 442 Ocean freshwater budgets. *Journal of Geophysical Research: Biogeosciences*, 112(4).  
 443 <https://doi.org/10.1029/2006JG000354>
- 444 Howell, S. E.L., Babb, D. G., Landy, J. C., Moore, G. W. K., Montpetit, B., & Brady, M. (2023). A  
 445 Comparison of Arctic Ocean Sea Ice Export Between Nares Strait and the Canadian Arctic  
 446 Archipelago. *Journal of Geophysical Research: Oceans*, 128(4).  
 447 <https://doi.org/10.1029/2023JC019687>
- 448 Howell, Stephen E.L., Brady, M., & Komarov, A. S. (2022). Generating large-scale sea ice  
 449 motion from Sentinel-1 and the RADARSAT Constellation Mission using the Environment  
 450 and Climate Change Canada automated sea ice tracking system. *Cryosphere*, 16(3),  
 451 1125–1139. <https://doi.org/10.5194/tc-16-1125-2022>
- 452 Ionita, M., Scholz, P., Lohmann, G., Dima, M., & Prange, M. (2016). Linkages between  
 453 atmospheric blocking, sea ice export through Fram Strait and the Atlantic Meridional  
 454 Overturning Circulation. *Scientific Reports*, 6. <https://doi.org/10.1038/srep32881>
- 455 Komarov, A. S., & Barber, D. G. (2014). Sea Ice Motion Tracking From Sequential Dual-  
 456 Polarization RADARSAT-2 Images. *IEEE Transactions on Geoscience and Remote*  
 457 *Sensing*, 52(1), 121–136. <https://doi.org/10.1109/TGRS.2012.2236845>
- 458 Krumpen, T., Gerdes, R., Haas, C., Hendricks, S., Herber, A., Selyuzhenok, V., et al. (2016).  
 459 Recent summer sea ice thickness surveys in Fram Strait and associated ice volume fluxes.  
 460 *Cryosphere*, 10(2), 523–534. <https://doi.org/10.5194/tc-10-523-2016>
- 461 Kwok, R. (2004). Fram Strait sea ice outflow. *Journal of Geophysical Research*, 109(C1),  
 462 C01009. <https://doi.org/10.1029/2003JC001785>

- 463 Kwok, R. (2009). Outflow of Arctic Ocean sea ice into the Greenland and Barent Seas: 1979-  
 464 2007. *Journal of Climate*, 22(9), 2438–2457. <https://doi.org/10.1175/2008JCLI2819.1>
- 465 Kwok, R. (2018). Arctic sea ice thickness, volume, and multiyear ice coverage: losses and  
 466 coupled variability (1958 – 2018). *Environmental Research Letters*, 13(10), 105005.  
 467 <https://doi.org/10.1088/1748-9326/aae3ec>
- 468 Kwok, R., & Rothrock, D. A. (1999). Variability of Fram Strait ice flux and North Atlantic  
 469 Oscillation. *Journal of Geophysical Research*, 104(C3), 5177–5189.
- 470 Kwok, R., Schweiger, A., Rothrock, D. A., Pang, S., & Kottmeier, C. (1998). Sea ice motion from  
 471 satellite passive microwave imagery assessed with ERS SAR and buoy positions. *Journal*  
 472 *of Geophysical Research*, 103(C4), 8191–8214. <https://doi.org/10.1029/97JC03334>
- 473 Landy, J., & Dawson, G. (2022). Year-round Arctic sea ice thickness from CryoSat-2 Baseline-D  
 474 Level 1b observations 2010-2020 (Version 1.0) [Data set].
- 475 Landy, J. C., Petty, A. A., Tsamados, M., & Stroeve, J. C. (2020). Sea Ice Roughness  
 476 Overlooked as a Key Source of Uncertainty in CryoSat-2 Ice Freeboard Retrievals. *Journal*  
 477 *of Geophysical Research: Oceans*, 125(5), 1–18. <https://doi.org/10.1029/2019JC015820>
- 478 Landy, J. C., Dawson, G. J., Tsamados, M., Bushuk, M., Stroeve, J. C., Howell, S. E. L., et al.  
 479 (2022). A year-round satellite sea-ice thickness record from CryoSat-2. *Nature*, 609(7927),  
 480 517–522. <https://doi.org/10.1038/s41586-022-05058-5>
- 481 Lique, C., Treguier, A. M., Scheinert, M., & Penduff, T. (2009). A model-based study of ice and  
 482 freshwater transport variability along both sides of Greenland. *Climate Dynamics*, 33(5),  
 483 685–705. <https://doi.org/10.1007/s00382-008-0510-7>
- 484 Liston, G. E., Itkin, P., Stroeve, J., Tschudi, M., Stewart, J. S., Pedersen, S. H., et al. (2020). A  
 485 Lagrangian Snow-Evolution System for Sea-Ice Applications (SnowModel-LG): Part I—  
 486 Model Description. *Journal of Geophysical Research: Oceans*, 125(10).  
 487 <https://doi.org/10.1029/2019JC015913>
- 488 Provost, C., Sennéchaël, N., Miguet, J., Itkin, P., Rösel, A., Koenig, Z., et al. (2017).  
 489 Observations of flooding and snow-ice formation in a thinner Arctic sea-ice regime during  
 490 the N-ICE2015 campaign: Influence of basal ice melt and storms. *Journal of Geophysical*  
 491 *Research: Oceans*, 122(9), 7115–7134. <https://doi.org/10.1002/2016JC012011>
- 492 Rabe, B., Dodd, P. A., Hansen, E., Falck, E., Schauer, U., MacKensen, A., et al. (2013). Liquid  
 493 export of Arctic freshwater components through the Fram Strait 1998–2011. *Ocean*  
 494 *Science*, 9(1), 91–109. <https://doi.org/10.5194/os-9-91-2013>
- 495 Ricker, R., Girard-Ardhuin, F., Krumpfen, T., & Lique, C. (2018). Satellite-derived sea ice export  
 496 and its impact on Arctic ice mass balance. *The Cryosphere*, 12(9), 3017–3032.  
 497 <https://doi.org/10.5194/tc-12-3017-2018>
- 498 Serreze, M. C., Barrett, A. P., Slater, A. G., Woodgate, R. A., Aagaard, K., Lammers, R. B., et  
 499 al. (2006). The large-scale freshwater cycle of the Arctic. *Journal of Geophysical Research:*  
 500 *Oceans*, 111(11), 1–19. <https://doi.org/10.1029/2005JC003424>
- 501 Sirevaag, A., & Fer, I. (2009). Early spring oceanic heat fluxes and mixing observed from drift  
 502 stations north of Svalbard. *Journal of Physical Oceanography*, 39(12), 3049–3069.  
 503 <https://doi.org/10.1175/2009JPO4172.1>
- 504 Smedsrud, L. H., Halvorsen, M. H., Stroeve, J. C., Zhang, R., & Kloster, K. (2017). Fram Strait  
 505 sea ice export variability and September Arctic sea ice extent over the last 80 years.  
 506 *Cryosphere*, 11(1), 65–79. <https://doi.org/10.5194/tc-11-65-2017>

- 507 Spreen, G., Kern, S., Stammer, D., & Hansen, E. (2009). Fram Strait sea ice volume export  
 508 estimated between 2003 and 2008 from satellite data. *Geophysical Research Letters*,  
 509 36(19), 1–6. <https://doi.org/10.1029/2009GL039591>
- 510 Spreen, G., de Steur, L., Divine, D., Gerland, S., Hansen, E., & Kwok, R. (2020). Arctic Sea Ice  
 511 Volume Export Through Fram Strait From 1992 to 2014. *Journal of Geophysical Research:  
 512 Oceans*, 125(6). <https://doi.org/10.1029/2019JC016039>
- 513 de Steur, L., Hansen, E., Gerdes, R., Karcher, M., Fahrbach, E., & Holfort, J. (2009).  
 514 Freshwater fluxes in the East Greenland Current: A decade of observations. *Geophysical  
 515 Research Letters*, 36(23), 1–5. <https://doi.org/10.1029/2009GL041278>
- 516 Stroeve, J., Liston, G. E., Buzzard, S., Zhou, L., Mallett, R., Barrett, A., et al. (2020). A  
 517 Lagrangian Snow Evolution System for Sea Ice Applications (SnowModel-LG): Part II—  
 518 Analyses. *Journal of Geophysical Research: Oceans*, 125(10).  
 519 <https://doi.org/10.1029/2019JC015900>
- 520 Stroeve, J. C., Schroder, D., Tsamados, M., & Feltham, D. (2018). Warm winter, thin ice?  
 521 *Cryosphere*, 12(5), 1791–1809. <https://doi.org/10.5194/tc-12-1791-2018>
- 522 Sumata, H., Lavergne, T., Girard-Ardhuin, F., Kimura, N., Tschudi, M. A., Kauker, F., et al.  
 523 (2014). An intercomparison of Arctic ice drift products to deduce uncertainty estimates.  
 524 *Journal of Geophysical Research: Oceans*, 119, 4887–4921.  
 525 <https://doi.org/10.1002/2013JC009724>
- 526 Sumata, H., de Steur, L., Gerland, S., Divine, D. V., & Pavlova, O. (2022). Unprecedented  
 527 decline of Arctic sea ice outflow in 2018. *Nature Communications*, 13(1).  
 528 <https://doi.org/10.1038/s41467-022-29470-7>
- 529 Sumata, H., de Steur, L., Divine, D. V., Granskog, M. A., & Gerland, S. (2023). Regime shift in  
 530 Arctic Ocean sea ice thickness. *Nature*, 615(7952), 443–449.  
 531 <https://doi.org/10.1038/s41586-022-05686-x>
- 532 Tschudi, M. A., Meier, W. N., Stewart, J. S., Fowler, C., & Maslanik, J. A. (2019). *Polar  
 533 Pathfinder Daily 25 km EASE-Grid Sea Ice Motion Vectors, Version 4*. Boulder, Colorado,  
 534 USA. <https://doi.org/https://doi.org/10.5067/INAWUWO7QH7B>
- 535 Vinje, T., Nordlund, N., & Kvambekk, A. (1998). Monitoring ice thickness in Fram Strait. *Journal  
 536 of Geophysical Research*, 103(C5), 10,437-10,449.
- 537 Warren, S. G., Rigor, I. G., Untersteiner, N., Radionov, V. F., Bryazgin, N. N., Aleksandrov, Y. I.,  
 538 & Colony, R. L. (1999). Snow Depth on Arctic Sea Ice. *Journal of Climate*, 12, 1814–1829.  
 539 [https://doi.org/10.1175%2F1520-  
 540 0442%281999%29012%3C1814%3ASDOASI%3E2.0.CO%3B2](https://doi.org/10.1175%2F1520-0442%281999%29012%3C1814%3ASDOASI%3E2.0.CO%3B2)
- 541 Zhang, J., Lindsay, R., Schweiger, A., & Steele, M. (2013). The impact of an intense summer  
 542 cyclone on 2012 Arctic sea ice retreat. *Geophysical Research Letters*, 40(4), 720–726.  
 543 <https://doi.org/10.1002/grl.50190>
- 544
- 545